

Mathematical Modeling and Optimization of Polymer Composite Pine Fins

S. Ayyad

Faculty of Engineering, Shebin El-Koom, Egypt.

Abstract:

Thermal basins are used in the industry, which consists of arrays of fins, which are designed in various forms for thermal packaging of electronic devices. The best design for the consumption of thermal basins for less mass and less energy should include certain considerations, such as the choice of engineering materials and the provision of high fiber thermal conductivity fibers that are made of carbon fiber and graphite to increase thermal conductivity. This use is better than using conventional materials such as aluminum and copper.

In order to achieve optimum objectives for engineering applications, an optimum design for the use of these thermal banks should be based on a precise balance between the best thermal design and the economic reduction of material consumption and minimal energy flow.

The current research presents a systematic study of the thermal performance of an air cooled heat sink designed by high thermal conductivity PPS polymer. A nested pin fin set has been used to design and improve such a natural heat sink that is cooled by air.

Keywords: modeling; optimization; pin fins; ANSYS; composite material

I. INTRODUCTION

Modern industries require electronic products to always maintain cooling methods to counter the heat resulting from use. This requires the use of new technologies and engineering materials. This has led scientists and designers to develop polymer compounds using carbon fiber as well as graphite fillings to increase thermal conductivity. These materials are an alternative to conventional metals such as aluminum and copper in the manufacture of heat exchangers. Heat tolerances and improved filler size of polymers are significantly different depending on the type and preparation of the material. Polymer compounds can be manufactured to reach the required thermal conductivity values based on thermal requirements [1]. This results and is achieved by controlling the dimensions and the direction of the fill.

The use of polymer-mounted fins on metals has important advantages of obtaining less manufacturing power as well as flexibility in the manufacturing stages, and easy assembly and weight control.

Polymers are used in difficult areas such as electronics under the hood because they are non-corrosive because their thermal performance in heat-cooled air basins is often limited by external thermal resistance so that the fine performance of the thermally conductive polymer fins can be achieved to achieve better thermal performance of copper and heat-cooled aluminum Air.

Previous research has included this problem related to cooling electronics. These studies, including the use of air cooling systems [2-7], were designed on liquid cooling [8-10]. Other studies have used the heat sink (fins), including studies that used the bundle of ball networks [11, 12], including piezoelectric [13] and thermal acoustic motors [14]. Other research has used the modeling behavior of electronic components [15-18].

In this study we used the ANSYS code to predict the performance of dorsal fin arrays for different forms. The expected results can be used to refer to the pin fin collection that works better under the same conditions, and the fin diameter to the center-to-center divergence that can perform best.

II. THE FINITE ELEMENT METHOD

In this study, the ANSYS program uses strong and powerful computational fluid dynamics (CFD) for thermal management of electronics. This use is considered the best for its advantages in improving productivity, which makes the design faster in establishing and simulating electronic cooling models for integrated circuit packages, printed circuit boards and complete electronic systems.

To obtain any better way to access any program health and experimental results for temperature distribution in polymer pin compound fin immersed in water obtained by Zhnegguo et

al. [19] Used. Various elements of fin dimensions, as well as natural convection in water, were combined to produce vital numbers in the range 1.3-4.3. The differences in pin fin temperature distribution and total heat flow rates can be predicted using ANSYS Mechanical ADPL 16.0 and compared to the experimental study [19].

For easy use of the analysis procedure, 2D modeling was used only. The geometry of this problem is presented in Fig. 1.

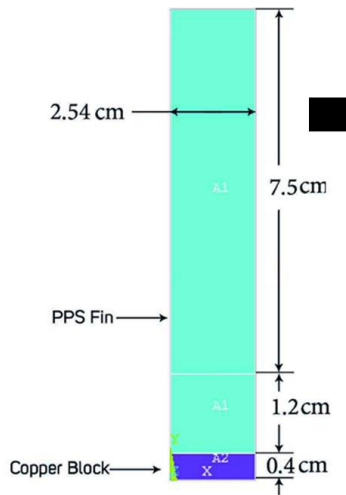


Fig. 1. Top view of PPS composite pin fin

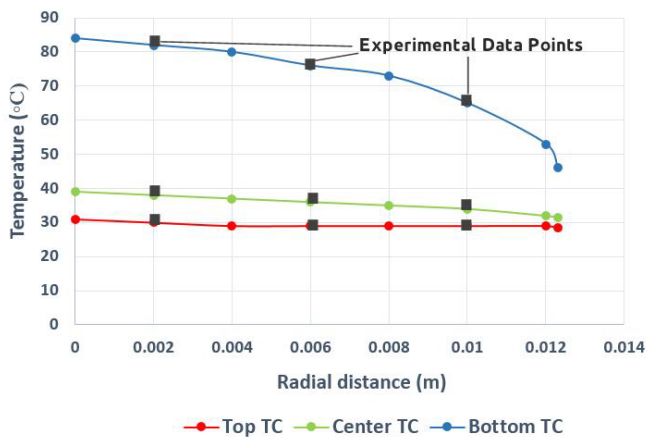


Fig. 2. Validation curve for a heat transfer rate of 27.4 W ($kz=13$ W/m.K, $Kr=2$ W/m.K, $Ta=28.1$ °C, $q''=54101.1$ W/m²)

During these experimental results, the power supply of 27.4 watts was obtained as black squares. The linear curves in Fig. 2 show numerical results obtained in advance using ANSYS 16.0 2D axiymmetric models. , A good agreement between the experimental and numerical results is achieved at 9 points in the tested PPS compound tested with the W / mK axial conduction value and the radial conduction value of 2 W / mK at 0.5 cm fin height, showing the results reaching the largest variation In the radial temperature, the agreement between the numerical and experimental excess temperatures is within 1.2%.

III. RESULTS AND DISCUSSION

Figure 3 shows the 3D CFD structure designed in Ansys Icepak 16.0. The dimensions of the metal body are determined using standard dimensions of the common body by hollow blocks as well as internal parts represented as broken blocks. During modeling, all parts within the structure are designed as standard components and the final micro dimensions are obtained by measurement.

The CPU is designed as a 40-watt dimension area. And a 45 x 45 mm section of the CPU is commercially available AMD CPU. Similar to the motherboard, has a number of chips that are identical to zero thickness with uniformly generated heat.

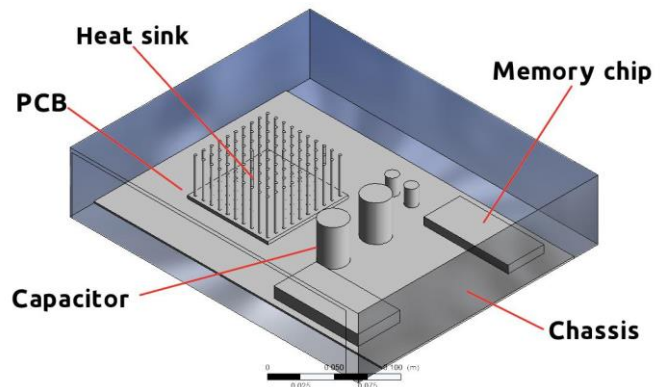


Fig. 3. Schematic illustration of the 3D chassis model

TABLE I. CABINET DIMENSIONS

| Cabinet dim. | X | Y | Z |
|--------------|-------|----|-------|
| X-Start (mm) | 0 | 0 | -25.4 |
| Length (mm) | 304.8 | 85 | 254 |

Selecting both minimum and maximum z sides of the cabinet as the opening, taking the inlet air speed as 2 m/sec.

TABLE II. MOTHERBOARD PCB MODELLING

| PCB dim. | X | Y | Z |
|--------------|-------|--------|-------|
| X-Start (mm) | 0 | 0 | 0 |
| Length (mm) | 304.8 | 1.5875 | 203.2 |

S. Ayyad “Mathematical Modeling and Optimization of Polymer Composite Pine Fins”

Enter the dimension values as shown in table II, take the following material FR-04_Ref (material properties as shown in table III), and enter the power supplied of 5 Watt.

TABLE III. PHYSICAL PROPERTIES OF FR-4_REF MATERIAL

| | |
|---|------------------------------------|
| Density = 1250 kg/m ³ | Specific heat = 1300 J/kg.K |
| Conductivity type = Isotropic | Conductivity = 0.3 W/m.K |

The assembly consists of Al CPU socket used to ensure proper mounting of the CPU with 50×50mm and CPU chip with 45×45mm dissipating 40 W.

TABLE IV. CPU CABINET DIMENSIONS

| CPU dim. | X | Y | Z |
|-------------|----|-------|----|
| Start (mm) | 70 | 5.08 | 90 |
| Length (mm) | 45 | 0.254 | 45 |

TABLE V. SOCKET DIMENSIONS

| Socket dim. | X | Y | Z |
|-------------|----|--------|----|
| Start (mm) | 60 | 1.5875 | 90 |
| Length (mm) | 50 | 3.4925 | 50 |

Enter the dimension values as shown in table VI, take the following material Ceramic material (material properties as shown in table VII), enter the radius as 12.7 mm, and height as 38.1mm.

TABLE VI. CAPACITOR DIMENSIONS

| Capacitor dim. | X | Y | Z |
|-------------------|-----|--------|----|
| Center Point (mm) | 180 | 1.5875 | 85 |

TABLE VII. PHYSICAL PROPERTIES OF THE CERAMIC MATERIAL

| | |
|---|----------------------------------|
| Density = 3970 kg/m ³ | Specific heat = 61 J/kg.K |
| Conductivity type = Isotropic | Conductivity = 15 W/m.K |

Enter the dimension values as shown in table VIII, take the following material Poly-Phenylene Sulphide composite PPS (material properties as shown in table IX), enter the pin radius as 1.65mm, height as 45mm number of fins as 10, base plate thickness as 3mm and height as 6mm.

TABLE VIII. HEAT SINK DIMENSIONS

| Heat Sink dim. | X | Y | Z |
|----------------|------|-------|----|
| Start (mm) | 50.8 | 5.334 | 70 |
| Length (mm) | 85 | 0 | 85 |

TABLE IX. PHYSICAL PROPERTIES OF PPS MATERIAL

| | |
|---|---|
| Density = 1700 kg/m ³ | Specific heat = 900 J/kg.K |
| Conductivity type = Orthotropic | Conductivity: kx = kz = 4 W/m.K, and ky = 20 W/m.K |

ANSYS Icepak automates the mesh generation procedure, but enables you to customize the meshing parameters in order to refine the mesh and optimize trade-offs between computational cost and solution accuracy.

Grid elements represent a smaller part of the proximal object to show the range of thermal gradients and velocity near the object's boundaries. On the other hand, open spaces between objects are designed with large elements for the purpose of reducing costs to lower values as shown in Figure 4.

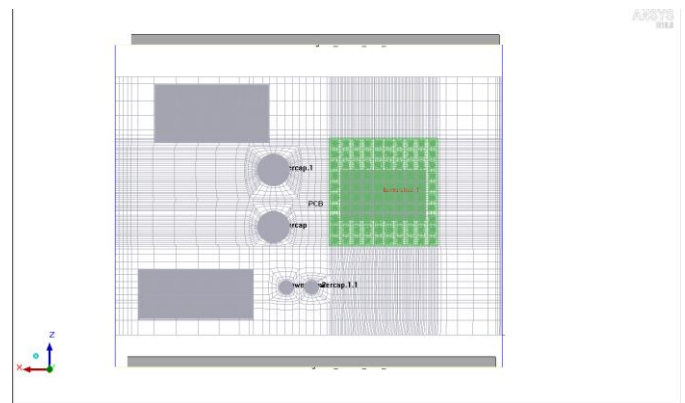


Fig. 4. Top view of 3D chassis meshing

The temperature contour for the chassis model was obtained by CFD Post-processing software 16.0 as shown in Fig. 5 showing heat sink temperature range of maximum temperature of about 81°C and minimum temperature of 36°C, the ideal working temperature for Core i7 CPU processor is 34-40°C.

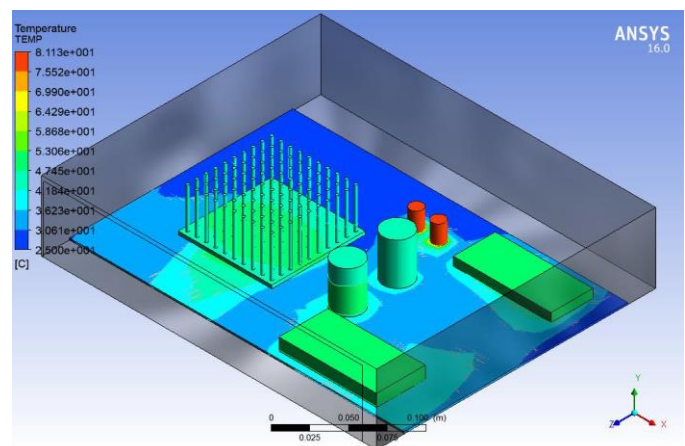


Fig. 5. Temperature contour using PPS heat sink (k=20 W/mK)

Using the same dimensions of CFD chassis, heat sink, boundary conditions and meshing parameters but changing heat sink material to aluminum and copper to compare with the performance of PPS heat sink, it's noticed that cooling rates of aluminum and copper heat sink are higher than PPS heat sink,

and the cooling rate of copper is higher than aluminum as shown in Fig. 6.

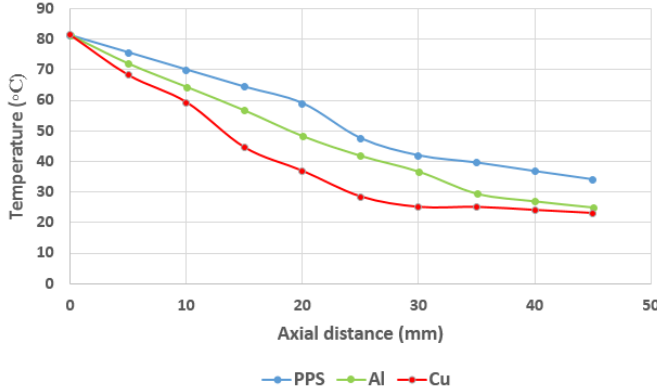


Fig. 6. Temperature variation along axial distance of the pin fin

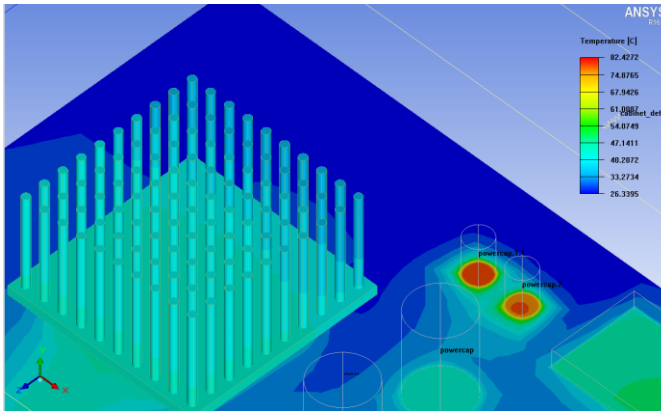


Fig. 7. Temperature contour for inline PPS heat sink

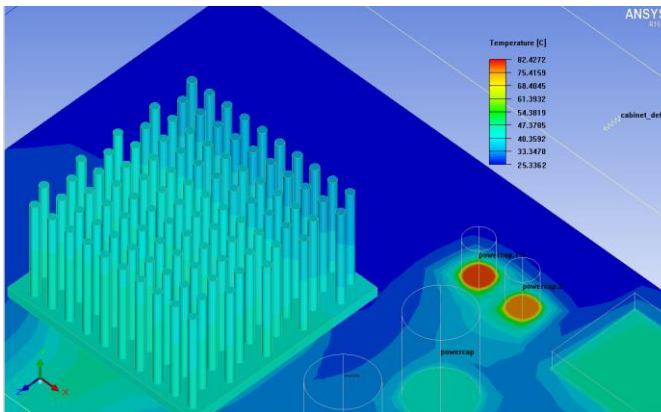


Fig. 8. Temperature contour for staggered PPS heat sink

It's noticed from the temperature contours shown in Fig. 7 and Fig. 8 that cooling rates of staggered configuration is slightly higher than the inline configuration and can perform better in transferring and dissipating heat, the cooling rate is shown in Fig. 9.

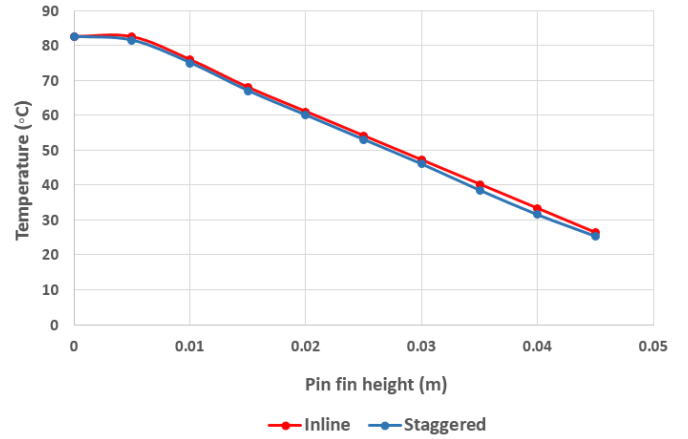


Fig. 9. Cooling rates of staggered and inline pin fin configuration

The heat sink that is fully cooled covers only part of the target. The new design leads to the formation of the best thermal sink solution for the application and benefits the overall design of the system. Numerous variables such as the dimensions of the base plate, convection, heat source dimensions, pin dimensions, fin or interlocking fins, fluid characteristics and material properties have been used to improve heat sink performance to meet specific design criteria.

Taking constraint function that the global maximum temperature of the 3D Chassis is 45°C and the objective function is to minimize thermal resistance. After running optimization, it appears that the thermal resistance decreases, as the fin radius increases as shown in Fig. 10.

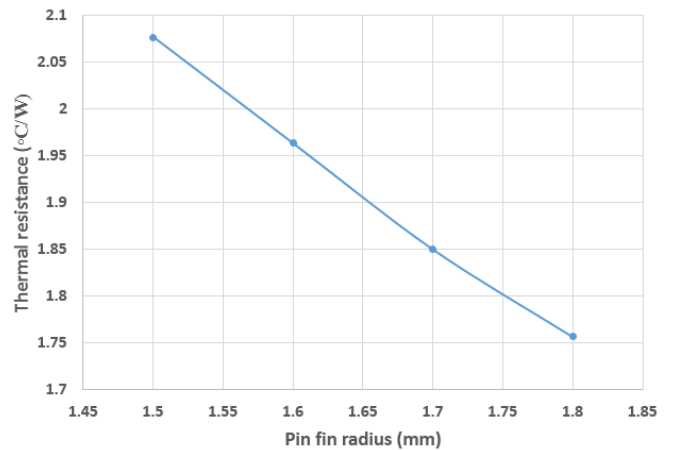


Fig. 10. Effect of Pin Fin Radius on Thermal Resistance

It's noted as shown in Fig. 11 that with increasing pin height, the thermal resistance decreases until it reaches the value of 5cm and then, it increases. It's noted also as shown in Fig. 12 that, the thermal resistance decreases steadily, as the number of fins increases from 6 to 14 fins; after that the number of fins has no significant effect on thermal resistance.

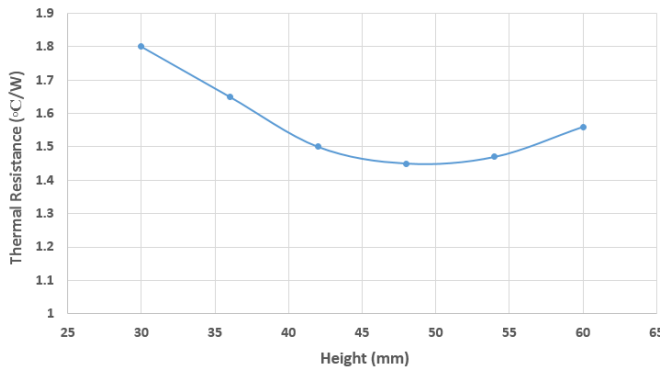


Fig. 11. Effect of Pin Fin Height on Thermal Resistance

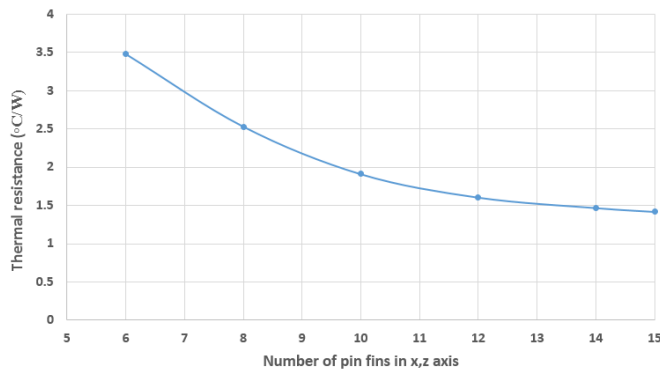


Fig. 12. Effect of number of fins on thermal resistance

Figure 13 shows the significant difference in the heat transfer coefficient in the array with the fin height with a subset of PPS, aluminum and thermal copper.

It is also shown that there can be a "perfect" height of the fin for each composition of fin diameter spacing. As the heat transfer coefficient of the matrix increases significantly, the fin height is gradually approaching and decreasing gradually as this elevation value is exceeded.

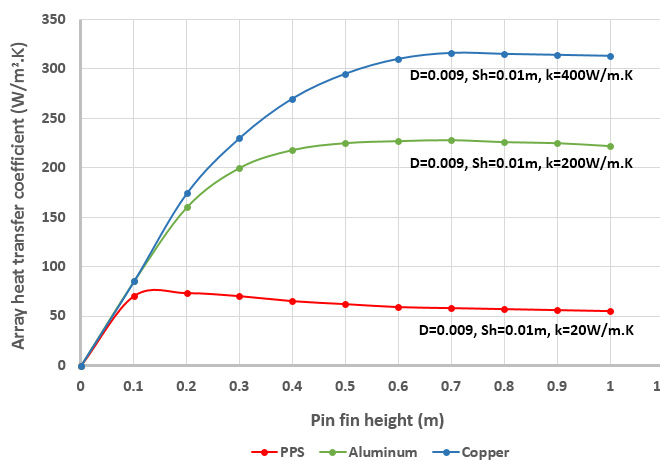


Fig. 13. Natural Convection Array Heat Transfer Coefficient Variation with Fin Conductivity and Height – Optimally Spaced Fins ($L= 0.1m$, $W = 0.1m$, $\theta_b=25K$)

Focusing first on the PPS fins, Fig. 13 shows that when the fin height equal 12cm, the thermal performance of the PPS pin fin array attains a peak value of $73 \text{ W/m}^2.K$ and then flattens out; however the aluminum heat sink thermal performance remains comparable to copper up to fin heights of 15cm. It may also be noted that with fin heights, up to 5cm, Fig. 13 shows that there is essentially no difference in the array heat transfer coefficients for these three materials and only relatively modest differences up to 10cm fin heights.

Owing to the relatively high thermal conductivity of copper and the resulting high fin efficiency for relatively tall fins, Fig. 13 displays a steady increase in the thermal performance of the copper pin fin array up to fin heights of 75cm and heat transfer coefficients of $320 \text{ W/m}^2.K$, while the aluminum pin fin array peaks at a value of $230 \text{ W/m}^2.K$.

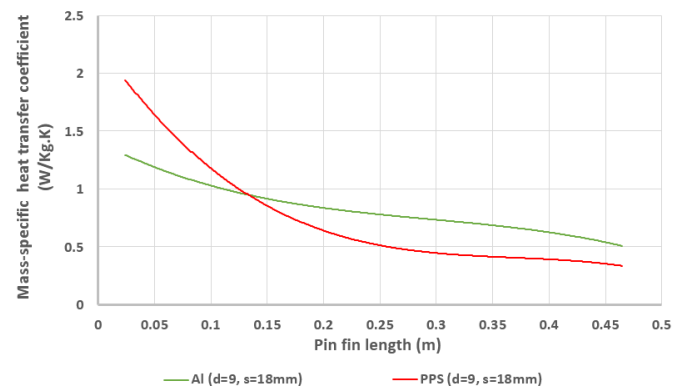


Fig. 14. Mass-specific heat transfer coefficient variation with pin fin height, thermal conductivity and diameter for aluminum and PPS heat sinks

The heat transfer rate per unit mass of the aluminum and the polymer composite polyphenylene sulphide heat sinks is depicted in Fig. 14. The figure indicates that for both materials, the h_m decreases monotonically with fin height.

When fin height is greater than 13 cm, the fin efficiency of the PPS is shown to result in almost constant heat transfer rates, although the physical surface area is large and the mass-based heat transfer coefficient is significantly reduced. It is clear that the aluminum heat sink faces a more efficient fin reduction, resulting in lower mass-based heat transfer values and values higher than PPS fins for elevations greater than 15 cm.

IV. .CONCLUSION

Thermal PPS thermocouples are found to provide thermal performance similar to those achieved with aluminum heat basins up to heights of approximately 5 cm. But the yield value was found to be three times greater than the value of the corresponding aluminum array for the optimal array design for the material with a minimum fin diameter of 0.9 cm and a spacing of 1 cm.

PPS composite pin fin heat sink can be used for natural convection air cooled microprocessor and surface mount components with reduced mass, and better matched CTE.

Moldability and lower cost provide significant advantages of using thermally conductive PPS composites for heat sinks.

Cooling rate as high as 16 W can be achieved at 10×10 cm base at temperature rise of 25 K above 45°C ambient temperature using optimized free convection air cooled PPS (20 W/m.K) pin finned heat sink. Thermal performance is comparable to aluminum pin finned heat sink up to fin heights of 5 cm.

Many parameters can be taken into consideration to make a design optimization for the heat sink such as fin-material, number of fins, fin-configuration, diameter, height, and air velocity. Based on the results, the following conclusions are drawn:

1. Staggered alignment performs better than in-line alignment.
2. The size and corresponding material cost are more for in-line alignment.
3. The thermal performance is improved with increasing number of fins.
4. The Total convective surface area increases with increasing the fin height.
5. Larger heat sink surface area will improve cooling, but may increase the cost.
6. Increasing the base-plate thickness distributes heat more uniformly to the fins if the CPU package is smaller than the heat sink, but increases weight.
7. The interface material can have a significant effect on assembly costs as well as on thermal resistance.
8. Thicker fins provide more structural integrity and may be easier to manufacture, but increase the weight for a given thermal resistance.
9. Copper fin gives the best performance, and if the weight of the heat sink is a constraint, the aluminum fin would be preferable.

The results indicate that some fin sections have different PPS values across different planes. Therefore, the following studies will be the study of finite fin model modeling with variable conductivity along the circumference of the pinch fin. This will help to understand the effect of truly anisotropic thermal conductivity on the total pin transfer rate and the heat distribution.

REFERENCES

- [1] D. Hansen, and G. A. Bernier, “Thermal conductivity of polyethylene: the effects crystal size, density, and orientation on the thermal conductivity,” *Polymer Engineering and Science*, vol. 12, no. 3, pp. 204, 1972.
- [2] Gary Shives et. al., “Comparative thermal performance evaluation of graphite/epoxy fin heat sinks,” *Proceedings IThERM 2004*, pp. 410-417.
- [3] Xuejiao Hu; Linan Jiang; and Goodson, K.E, “Thermal conductance enhancement of particle-filled thermal interface materials using carbon nanotube inclusions, Thermal and Thermomechanical Phenomena in Electronic Systems,” *ITHERM 2004, The Ninth Intersociety Conference on 1-4*, pp 63 – 69, vol. 1, June 2004.
- [4] O. Braunshtein, H. Kalman, A. Ullmann, “Performance and optimization of air cooled composed fin arrays,” *Heat Transfer Engineering* 25 (4), pp. 4–12, 2013.
- [5] C. Bougriou et al., “Measurement of the temperature distribution on a circular plane fin by infrared thermography technique,” *Applied Thermal Engineering* 24 (5–6), pp. 813–825, 2013.
- [6] S.C. Lin, and C.A. Chou, “Blockage effect of axial-flow fans applied on heat sink assembly,” *Applied Thermal Engineering* 24 (16), pp. 2375–2389, 2012.
- [7] B.E. Short Jr., D.C. Price, and P.E. Raad, “Design of cast pin fin cold walls for air cooled electronics systems,” *Journal of Electronic Packaging, Transactions of the ASME* 126 (1), pp. 67–73, 2012.
- [8] C.J. Shih, and G.C. Liu, “Optimal design methodology of plate-fin heat sinks for electronic cooling using entropy generation strategy,” *IEEE Transactions on Components and Packaging Technologies* 27 (3), pp. 551–559, 2012.
- [9] T.K. Aldoss, M.A. Al-Nimr, and M.A. Hader, “Using capsulated liquid metal fins for heat transfer enhancement,” *Journal of Enhanced Heat Transfer* 11 (2), pp. 151–160, 2012.
- [10] W.H. Hsieh et al., “Experimental investigation of heat-transfer characteristics of aluminum-foam heat sinks,” *International Journal of Heat and Mass Transfer* 47 (23), pp. 5149–5157, 2012.
- [11] A. Elbanhawy, “High-density power package for the PC market,” *Power Electronics Technology* 30 (11), pp. 48–55, 2010.
- [12] G. Peng, and M. Ishizuka, “Numerical simulation of heat dissipation from a plastic ball grid array package in a thin flat box: Effects of some operative and geometric parameters,” *Numerical Heat Transfer; Part A: Applications* 45 (1), pp. 67–83, 2010.
- [13] T. Acikalin et al., “Experimental investigation of the thermal performance of piezoelectric fans,” *Heat Transfer Engineering* 25 (1), pp. 4–14, 2004.
- [14] O.G. Symko et al., “Design and development of high-frequency thermoacoustic engines for thermal management in microelectronics,” *Microelectronics Journal* 35 (2), pp. 185–191, 2009.
- [15] L. Ghodoossi, and N. Ecrican, “Conductive cooling of triangular shaped electronics,” *Energy Conversion and Management* 45 (6), pp. 811–828, 2004.
- [16] V. Evely, P. Rodgers, and M.S. Hashmi, “Application of numerical analysis to the optimization of electronic component reliability screening and assembly processes,” *Journal of Materials Processing Technology* 155-156 (1–3), pp. 1788–1796, 2009.
- [17] V. Evely, P. Rodgers, and M.S. Hashmi, “Numerical prediction of electronic component operational temperature: A perspective,” *IEEE Transactions on Components and Packaging Technologies* 27 (2), pp. 268–282, 2008.
- [18] T.J. Goh et al., “Thermal investigations of microelectronic chip with nonuniform power distribution: Temperature prediction and thermal placement design optimization,” *Microelectronics International* 21 (3), pp. 29–43, 2008.
- [19] Z. Zhnegguo, X. Tao, and F. Xiaoming, “Experimental study on heat transfer enhancement of a helically baffled heat exchanger combined with three dimensional finned tubes,” *Applied Thermal Engineering* 24 (14-15), pp. 2293-2300, 2013.